

# Ultrasonic velocimetry in carbon black suspensions

Thomas Gibaud, Damien Frelat and Sébastien Manneville

Laboratoire de Physique, Université de Lyon - Ecole Normale Supérieure de Lyon, CNRS UMR 5672, 46 allée d'Italie, 69364 Lyon cedex 07, FRANCE (e-mail: sebastien.manneville@ens-lyon.fr)

Attractive colloidal gels display a solid-to-fluid transition as shear stresses above the yield stress are applied. This shear-induced transition is involved in virtually any application of colloidal gels. It is also crucial for controlling material properties. Still, in spite of its ubiquity, the yielding transition is far from understood, mainly because rheological measurements are spatially averaged over the whole sample. Here, the instrumentation of creep and oscillatory shear experiments with high-frequency ultrasound opens new routes to observing the local dynamics of opaque attractive colloidal gels. We show that the transition proceeds from the cell walls and heterogeneously fluidizes the whole sample with a characteristic time whose variations with applied stress suggest the existence of an energy barrier linked to the gelation process.

**Keywords:** colloidal gels, ultrasonic velocimetry, velocity profile, yielding.

## 1 INTRODUCTION

Colloidal particles with strong enough short range attraction are known to aggregate into fractal clusters that may form a space-spanning network leading to solid-like properties even at very low volume fractions [1]. In such a gel state, the system is kinetically arrested and displays non-ergodic features such as ultraslow relaxations, aging, and dynamical heterogeneities [2]. These glassy features have raised the issue of unifying the behaviour of colloidal gels and that of more concentrated amorphous jammed systems, e.g. colloidal glasses or concentrated emulsions [3].

Here, we focus on the stress-induced solid-to-fluid transition in carbon black suspensions, a totally opaque colloidal gel made of weakly attractive soot particles. We use high frequency ultrasound as a new tool to follow the local deformation and flow of the sample under an external stress. Both creep tests and oscillatory shear experiments show that, above a critical yield stress  $\sigma_y$ , (i) yielding proceeds from the cell walls in a spatially and temporally heterogeneous way and (ii) the time needed for total fluidization of the sample decreases exponentially with the applied shear stress.

## 2 MATERIALS AND METHODS

### 2.1 Carbon black gel preparation

Carbon black is widely used in industry, e.g. for coatings, printing, rubbers, tires, paints, or batteries [4]. These colloidal carbon particles result from partial combustion of fuel and are made of unbreakable aggregates of permanently fused nanometric primary particles. These aggregates have a typical diameter of 500 nm. When dispersed in a light mineral oil (from Sigma, density 0.838, viscosity 20 mPa.s) at a weight concentration of a few percents, carbon black particles (Cabot Vulcan XC72R of density 1.8) form a space-spanning network due to weakly attractive interactions of typical strength 30  $k_B T$  [3].

Our samples are prepared by vigorous mixing of 6% w/w carbon black particles into the mineral oil. Since the resulting gel is transparent to ultrasound, 1% w/w hollow glass microspheres of mean diameter 6  $\mu\text{m}$  (Spherical, Potters) are added in order to provide enough acoustic contrast (see below). The sample is further sonicated for 1 hour.

### 2.2 Ultrasonic echography under shear

In our experiments, classical rheology in Couette geometry is combined to ultrasonic echography in order to access local properties of the gel such as its velocity or deformation fields. Rheological measurements are performed in a smooth Plexiglas Couette cell (rotating inner cylinder radius 24 mm, gap width 1 mm, and height 30 mm) by a stress-imposed rheometer (Bohlin C-VOR 150, Malvern Instruments).

In creep experiments, we use ultrasonic speckle velocimetry (USV) as described in Ref. [5] to record temporally-resolved velocity profiles across the gap at about 15 mm from the cell bottom (Fig. 1a,b). USV is based on the interaction between ultrasound and micron-sized scatterers embedded in the gel (here, the glass microspheres that act as contrast agents). It gives access to the local velocity of the gel with a spatial resolution of about 40  $\mu\text{m}$ .

For oscillation experiments, we take advantage of ultrasonic echography in a new way by focusing on the spatiotemporal diagrams of the successive speckle signals (Fig. 1c-f). Indeed, the spatial variation of the speckle intensity provides crucial information on the local deformation of the sample. When pulses are sent with a sufficiently high repetition frequency  $f_{\text{prf}}$  compared to the oscillation frequency  $f$ , tracking the local oscillatory motion of the gel becomes possible (Fig. 1c and e). Here, we rather set  $f_{\text{prf}} = f$  so that the material is probed by ultrasound only once per oscillation period. Data analysis is then straightforward: if two successive speckle signals are fully correlated, then the gel is solid-like since it comes back exactly to the same

position every period (Fig. 1d). On the other hand, we interpret any significant degree of decorrelation in the speckle signal from one period to the other as the signature of fluid-like behaviour due to motions of the scatterers induced by local rearrangements inside the gel (Fig. 1f).

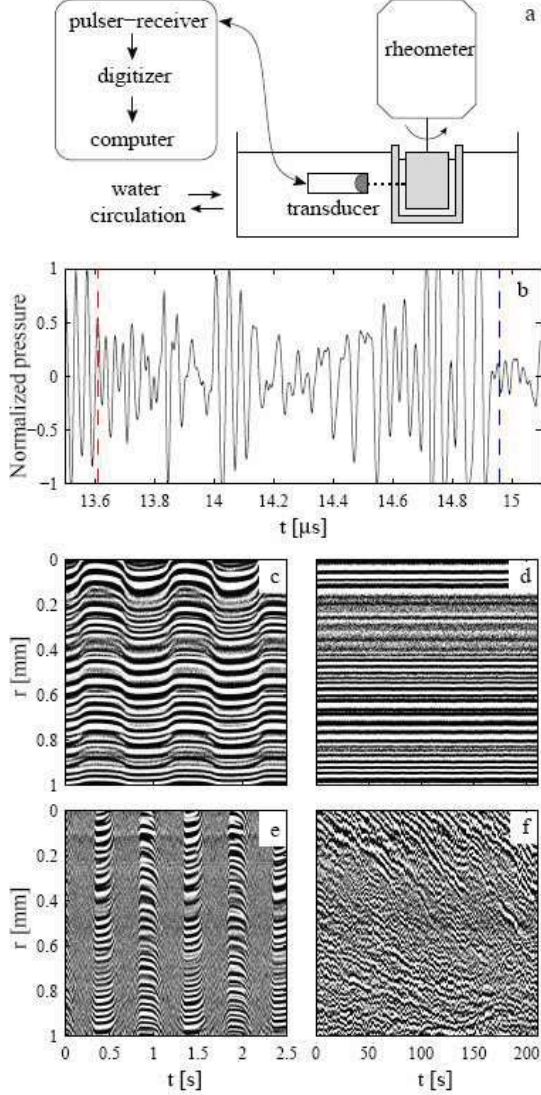


**Figure 1: Ultrasonic echography under shear.** (a) Schematic of the rheology experiment combined with USV. (b) Typical normalized pressure signal backscattered by glass microspheres embedded in a carbon black gel as a function of time after the incident pulse is emitted at  $t=0$  s. The times-of-flight corresponding to the positions of the stator and the rotor are indicated by a red and blue dashed line respectively. The corresponding gap is 1 mm. (c and d) Spatiotemporal diagrams of the normalized pressure signal during an oscillation experiment at  $f=1$  Hz and  $\sigma=15$  Pa. The pressure is coded in linear grey levels and plotted against the time at which the incident pulse is sent ( $x$ -axis) and the radial distance  $r$  to the rotor ( $y$ -axis). In (c), the pulse repetition frequency  $f_{\text{prf}}$  is 400 Hz, which is large enough to resolve the deformation due to the oscillations of the rotor, while in (d),  $f_{\text{prf}}=f=1$  Hz. (e and f). Same as in (c and d) but for a higher shear stress  $\sigma=30$  Pa.

The spatiotemporal tracking of the transition from correlated speckle signals (i.e. solid-like state) to decorrelated speckle signals (i.e. fluidized state) is made quantitative by using a threshold for the correlation coefficient of successive signals over small time windows, thus identifying the boundary between solid and fluid regions as a function of time up to a spatial resolution of 40  $\mu\text{m}$  (see Fig. 3d).

## 3 RESULTS

### 3.1 Creep experiments

Figure 2a gathers the results of creep experiments for a wide range of imposed shear stresses. The critical shear stress  $\sigma_y = 8.5 \pm 0.5$  Pa clearly separates two regimes. For  $\sigma < \sigma_y$ , the gel remains solid-like and does not flow, whereas for  $\sigma > \sigma_y$ , the sample eventually flows with a measurable shear rate, a transition known as the “viscosity bifurcation” in the soft glassy literature [6].

In order to get better insight into the fluidization process, we correlate the rheological measurements to the local velocity field  $v(r)$  measured with USV for the typical creep experiment at  $\sigma=10$  Pa shown in Fig. 2b. In the early stage where the shear rate slowly increases ( $t < 1500$  s), solid-body rotation is observed, i.e. the sample is in an unsheared solid-like state except for thin lubrication layers along the cell walls that allow the gel to slide as a solid block (Fig. 2c). The average velocity in the solid-like material slowly increases following the trend in the shear rate. At the beginning of the sharp upward bend in the shear rate, for  $1500 \text{ s} < t < 1800$  s, the bulk sample starts to experience a non-zero shear rate. Fluidization then proceeds in a spatially heterogeneous way. Indeed, in this regime, velocity profiles present a highly sheared region close to the rotor that coexists with a low-shear band next to the stator and whose size increases in time (Fig. 2d). Such a shear localization suggests that the gel progressively sticks to the cell walls and gets dragged along the rotor. The fluidized zone expands from the rotor until, for  $t \approx 1800$  s, the gel flows homogeneously without any apparent wall slip, as seen from the linear velocity profiles of Fig. 2e.

Our local measurements refute the simple scenario in which yielding occurs abruptly and homogeneously at  $\sigma_y$  and rather support a yielding mechanism that is heterogeneous in both space and time, where fluidization starts at the walls and propagates through the whole sample. Such front dynamics is reminiscent of heterogeneous nucleation as predicted by a phenomenological “fluidity” model [7]. The present experiment also allows us to define unambiguously a characteristic time  $\tau$  for fluidization as the time when homogeneous shear is first observed, e.g.  $\tau = 1850 \pm 100$  s for  $\sigma=10$  Pa. The fluidization time roughly corresponds to the inflection point in the shear rate curve.

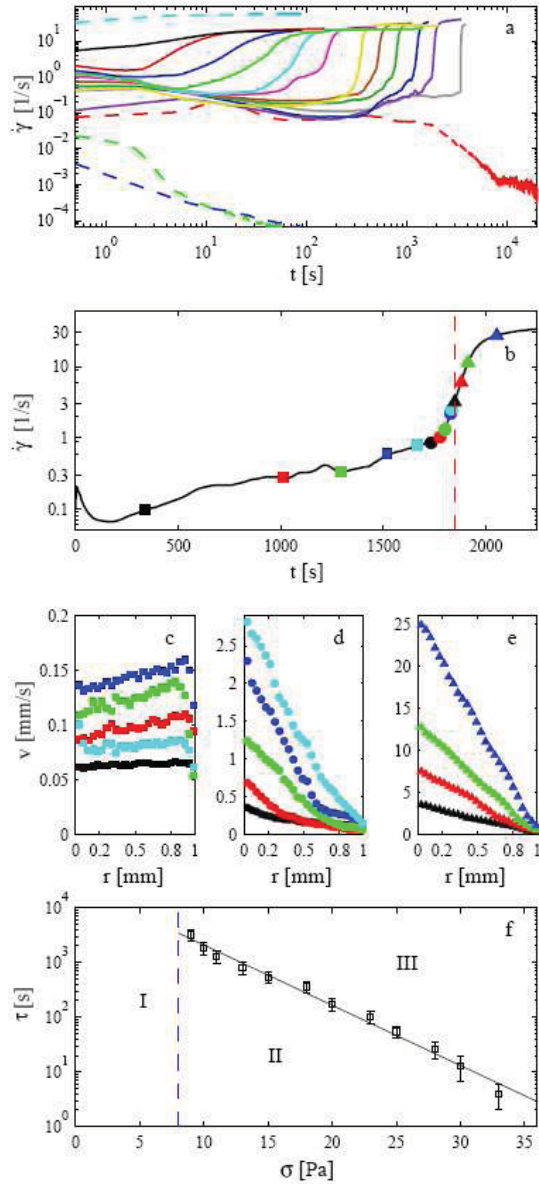


**Figure 2: Creep experiments** in a 6% w/w carbon black gel. (a) Temporal evolution of the shear rate for (from bottom to top)  $\sigma = 5, 7, 8, 9, 10, 11, 13, 15, 18, 20, 23, 25, 28, 30, 33$  and  $40$  Pa. (b-e) Combined rheological and USV measurements for  $\sigma = 10$  Pa. (b) Shear rate as a function of time. The red dashed line indicates the fluidization time  $\tau$  discussed in the text. (c, d, e) Instantaneous velocity profiles  $v(r)$  recorded with USV at the times shown in (b) using the same symbols. (f) The fluidization time  $\tau$  as a function of the applied shear stress  $\sigma$ . The black line is an exponential fit to the experimental data.

Fig. 2f sums up the behavior of our colloidal gel in creep experiments. Below  $\sigma_y$  (region I), the gel remains solid for all times, while above  $\sigma_y$ , the gel first undergoes solid-body rotation or shear localization for  $t < \tau$  (region II) and eventually flows homogeneously for  $t > \tau$  (region III). Remarkably, over the whole range  $\sigma = 8-33$  Pa, the fluidization time follows an exponential law:  $\tau \propto \exp(-\sigma/\sigma_0)$  where  $\sigma_0 = 4.0 \pm 0.2$  Pa. In other words, with  $\sigma_0 = k_B T/v$ ,

where  $v$  is some characteristic volume, this behaviour is equivalent to an Arrhenius law  $\tau \propto \exp(E(\sigma)/(k_B T))$ , where the energy barrier  $E(\sigma) = -\sigma v$  decreases linearly with the applied stress.

### 3.3 Oscillatory shear experiments

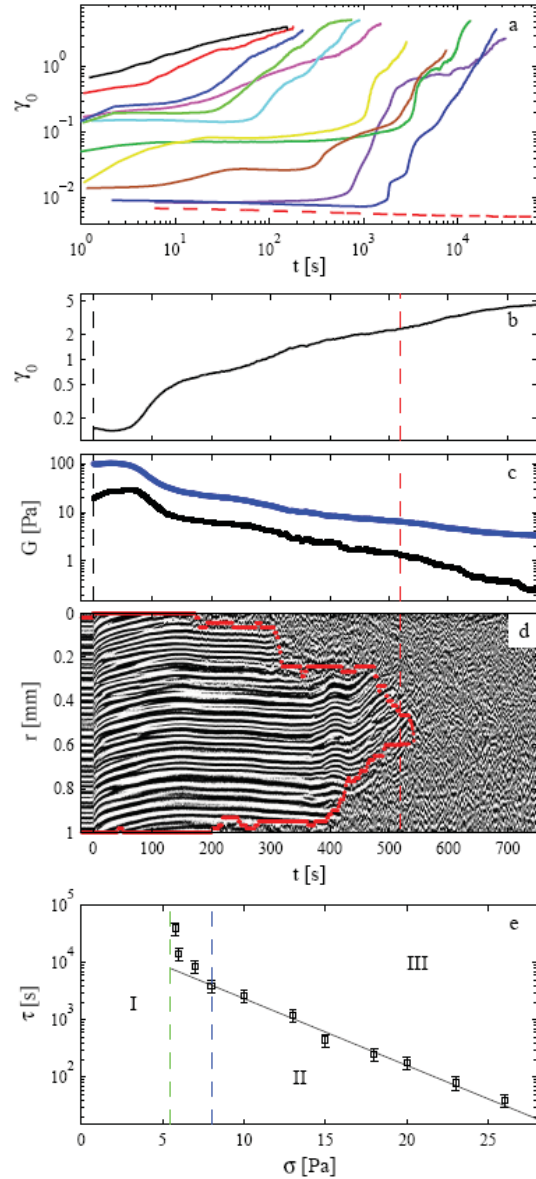


**Figure 3: Large amplitude oscillatory shear** experiments at  $f=1$  Hz in a 6% w/w carbon black gel. (a) Temporal evolution of the deformation amplitude  $\gamma_0$  for (from bottom to top)  $\sigma = 5, 5.8, 6, 7, 8, 10, 13, 15, 18, 20, 23, 26$  Pa. (b-d) Combined rheological and USV measurements for  $\sigma = 15$  Pa. (b)  $\sigma_0$  and (c)  $G'$  (black) and  $G''$  (blue) as a function of time. (d) Spatiotemporal diagram of the ultrasonic speckle signal coded in linear grey levels. The USV sampling frequency is equal to the oscillation frequency  $f=1$  Hz. Red dots indicate the boundary between solid-like and fluid-like regions. The red dashed line shows the time  $\tau$  at which 90% of the gel across the gap is fluidized. (e) The fluidization time  $\tau$  as a function of the stress amplitude  $\sigma$ . The black line is an exponential fit to the experimental data (only data above 8 Pa are considered in the fit).

In a second series of experiments, the gel is submitted to oscillatory shear stress of given amplitude  $\sigma$  and frequency  $f=1$  Hz. The strain amplitude  $\gamma_0$  is monitored and again, we observe that when  $\sigma$  is large enough  $\gamma_0$  eventually increases with time, suggesting that the sample becomes fluid over time (Fig. 3a,b). To confirm this scenario, we track the local deformation of the gel with USV (see Section 2.2). For  $\sigma < 5$  Pa, the gel indeed remains solid: no decorrelation of the ultrasonic speckle signals, i.e. no rearrangement within the gel, was observed during waiting times as long as  $10^5$  s. However, for stress amplitudes above 5 Pa, rearrangements and fluid-like behaviour are detected first close to the cell walls (see  $t \approx 100$ -300 s in Fig. 3d). The fluidized zone then progressively expands through the bulk material ( $t \approx 300$ -550 s) until the whole sample gets fluid ( $t > 550$  s).

It is important to note that fluidization does not have such a dramatic signature on  $\gamma_0$  under oscillatory stress as on the shear rate during creep tests. Moreover, as shown in Fig. 3c, the loss modulus is larger than the elastic modulus throughout the whole experiment. In view of the USV results, this can only be explained by the presence of lubrication layers at the walls. A naive interpretation of standard viscoelastic data would thus wrongly conclude that the sample is fluid as soon as stress is applied. Here simultaneous spatially-resolved measurements show that solid-fluid coexistence comes into play and reveal a highly heterogeneous fluidization pattern. In oscillation experiments, the fluidization time, defined as the time  $\tau$  for which 90% of the gel is in the fluid-like state, follows an exponential law  $\tau \propto \exp(-\sigma/\sigma_0)$  with  $\sigma_0 = 3.9 \pm 0.3$  Pa for  $\sigma > 8$  Pa (Fig. 3e). This is strikingly similar to the behaviour obtained in creep experiments (Fig. 2f). However, under an oscillatory stress of amplitude  $5 \text{ Pa} < \sigma < 8 \text{ Pa}$ , a strong departure from exponential behaviour is observed, pointing to a divergence at  $\sigma \approx 5.5$  Pa. In this stress range, no fluidization was observed during creep tests.

#### 4 DISCUSSION AND CONCLUSIONS

The creep tests and the oscillation experiments above have shown the benefit of local measurements in establishing a spatiotemporal scenario for yielding: fluidization is initiated at the walls and propagates into the entire sample within a characteristic time  $\tau$  that follows an Arrhenius law. Such a scaling provides evidence for the relevance of activated processes and barrier hopping in the context of yielding in colloidal gels. Although such ingredients have recently been incorporated into theoretical approaches based on mode-coupling theory [8] or on the shear-transformation zone (STZ) theory [9], local dynamical descriptions are still missing from microscopic models of the stress-induced solid-to-fluid transition.

To conclude, ultrasonic echography constitutes a versatile tool to follow yielding and fluidization in both space and time even in optically opaque materials. Its mesoscopic resolution of a few  $10 \mu\text{m}$  bridges the gap between microscopic imaging techniques and global rheological measurements. Indeed, coarse-grained models for soft glassy materials use local strains and stresses averaged over intermediate sizes [10,11], so that gathering information at a mesoscopic scale is a key issue for comparing experiments to such models. From the fundamental point of view, our observations not only emphasize the importance of activated processes in yielding but also reveal a complex interplay between boundaries and bulk dynamics.

#### REFERENCES

- [1] W. B. Russel, D. A. Saville, and W. R. Schowalter, *Colloidal Dispersions*, Cambridge University Press (New York), 1989.
- [2] L. Cipelletti et al., *Phys. Rev. Lett.* 84 (2000) 2275-2278.
- [3] V. Trappe et al., *Nature* 411 (2001) 772-775.
- [4] J.-B. Donnet, R. C. Bansal, and M.-J. Wang, *Carbon black: Science and technology*, Marcel Dekker Inc. (New York), 1993.
- [5] S. Manneville, L. Bécu, and A. Colin, *Eur. Phys. J. AP* 28 (2004) 361-373.
- [6] P. Coussot et al., *J. Rheol.* 46 (2002) 573-589.
- [7] G. Picard et al., *Phys. Rev. E* 66 (2002) 051501.
- [8] V. Kobelev and K. S. Schweizer, *Phys. Rev. E* 71 (2005) 021401.
- [9] M. L. Falk, J. S. Langer, and L. Pechenik, *Phys. Rev. E* 70 (2004) 011507.
- [10] L. Bocquet, A. Colin, and A. Ajdari, *Phys. Rev. Lett.* 103 (2009) 036001.
- [11] S. M. Fielding, M. E. Cates, and P. Sollich, *Soft Matter* 5 (2009) 2378-2382.